Characterizing the Polarimetric Response of the Daksha Space Telescope

Supervised Learning Project

Advait Mehla
Guide : Prof. Varun Bhalerao

Abstract

X-ray astronomy has come a long way since its beginnings via detectors launched on the nose cones of sounding rockets back in the 1950s. X-ray polarimetry, on the other hand, is a largely unexplored area within this otherwise mature field. With the launch of AstroSat in 2015, we have been able to obtain sensitive measurements of X-ray polarization data via the CZTI instrument onboard. For the proposed Daksha Space Telescope, we seek to create a software pipeline in Python, to perform polarization analysis with the data to be obtained from the on-board detectors. Daksha's high sensitivity and large field of view will make it the workhorse for high energy transient discovery and characterisation in the coming decade. To gauge the polarisation capabilities of Daksha, the team has developed a software pipeline to estimate the polarisation of GRBs. My work in this SLP has been aimed at understanding the methodology used, develop it further and validate it with various tests.

Contents

1 Introduction

Polarisation of photons is a fundamental property imparted by their electromagnetic wave nature. Photons are 'packets' of transversely oscillating, mutually perpendicular electric and magnetic fields. The direction in which the electric field is oriented is conventionally used to determine the polarisation.

While all photons have some polarisation, a beam of photons can have varying polarisation angles (PA). If the distribution of angles is uniform, the source is said to be unpolarised and have zero net polarisation. Otherwise, it is said to have some net polarisation. A polarised beam of light can be considered to be a superposition of a fraction which is completely polarised in a certain direction, and the rest which is completely unpolarised. This fraction is known as the polarisation fraction (PF).

X-ray astronomy deals with observation of astronomical objects in the high energy X-ray band of the spectrum. As the Earth's atmosphere is opaque to this band of energies, such observations are made using space telescopes in orbit. Historically, observations have also been made with high altitude balloons. In astronomical sources, generation of a non-zero net polarisation requires asymmetries in the geometry of the source or the magnetic field configuration of the system (Kaaret, 2014). Polarisation data thus carries a wealth of information about radiation generation processes and environments around astrophysical sources, information that otherwise cannot be probed directly.

Daksha is a proposed high-energy transients mission comprising of two satellites monitoring the entire sky in the 1 keV to 1MeV range. The primary goals of Daksha are to study the electromagnetic counterparts of gravitational waves, and prompt emission GRBs. Daksha is also designed to be an effective instrument for X-Ray polarimetry. This project is an effort to create a software pipeline in Python to perform polarisation analysis using data to be gathered from Daksha in the future and to also estimate the sensitivity and suitability of Daksha as a X-ray polarisation instrument.

2 Gamma-Ray Bursts

Gamma-ray bursts or GRBs are immensely energetic explosions that have been observed throughout the universe. They have durations lying anywhere between a few milliseconds and several minutes. After an initial flash of gamma rays, there is a longer-lived afterglow that is emitted at longer wavelengths, ranging from UV to radio waves. Daksha hopes to study these transients better and help unveil

Figure 1: *Artist's rendering of a GRB. Image Credit: Hubble Resource Gallery*

the progenitors of these explosions by making polarisation measurements from the initial, short-lived prompt-emission phase.

In spite of a wealth of detections exceeding 5000 over the past two decades, the emission mechanism is still largely unknown (Grossan et al., 2019). Accurate polarisation measurements provide a useful way to select or reject the various contesting theories, thus revealing new insights into the progenitors of these explosions.

2.1 Spectrum

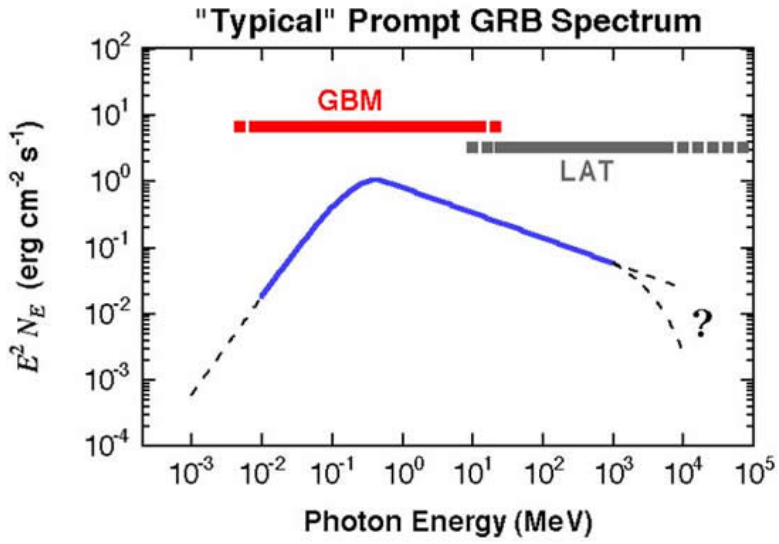

Figure 2: *A sample GRB spectrum. Image Credit: David Band*

The spectrum of GRBs is non-thermal. Typically, the spectral distribution peaks at a few hundred keV and has a long high energy tail. This spectrum is seen to vary significantly from one bust to another, but there is a phenomenological fit

known as the Band function (Band et al., 1993) that works well in most cases -

$$N_E(E) = A\left(\frac{E}{100\text{keV}}\right)^{\alpha}\exp\left(-\frac{E}{E_0}\right) \qquad ,(\alpha-\beta)E_0 \geq E$$
$$= A\left[\frac{(\alpha-\beta)E_0}{100\text{keV}}\right]^{\alpha-\beta}\exp(\beta-\alpha)\left(\frac{E}{100\text{keV}}\right)^{\beta} \qquad ,(\alpha-\beta)E_0 \leq E$$

Where E is in keV, α, β are dimensionless constants. When a GRB is detected, these parameters can be obtained from the observed spectrum.

3 Daksha

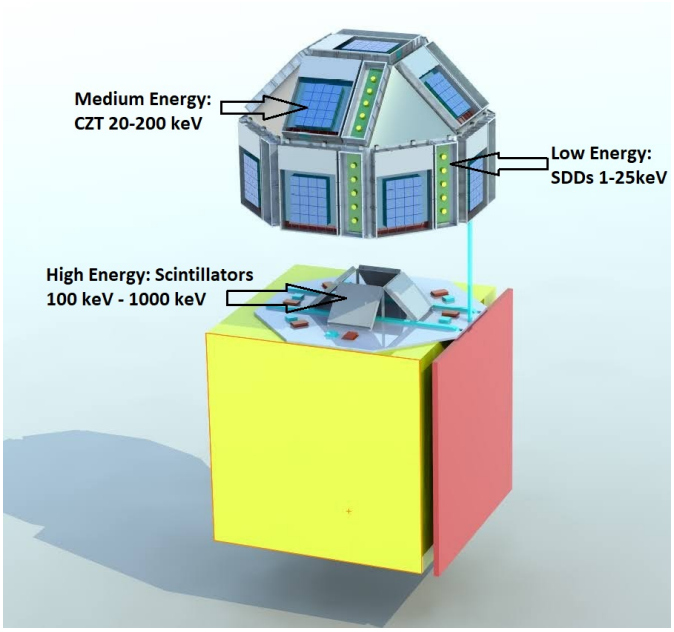

Figure 3: *Proposed design of Daksha. Image Credit: Gaurav Waratkar and the Daksha tea*m

Daksha is a proposed space telescope being developed by several Indian research institutes, with IITB leading the efforts. It will be an order of magnitude more sensitive than any existing mission. It will cover the energy range from 1 keV to 1 MeV, reaching a sensitivity higher than the Neil Gehrels Swift Observatory. Two satellites orbiting on opposite sides of Earth will ensure continuous coverage of the entire sky.

The workhorse for Daksha are sensitive pixelated Cadmium Zinc Telluride (CZT) detectors. Daksha will use 3.9 cm×3.9 cm×5 mm detectors, sensitive to an energy

range of $20-200$ keV. Each individual detector is divided into a 16×16 pixel array. Medium Energy (ME) packages will consist of 20 such detectors, and Daksha will have 17 such ME packages.

Daksha will thus have 340 CZT detectors onboard, compared to AstroSat/CZTIs 64 CZT detectors, which will allow us to perform polarisation analysis on detected X-ray transients. With more detectors, and a mission comprised of two satellites, Daksha is expected to have higher sky coverage than AstroSat. With its CZT detectors being in different orientations, it is not only expected to detect more transients than AstroSat, but also to help in quantifying any systematic errors in transient polarisation measurements, an advantage over the coplanar quadrants of AstroSat/CZTI.

3.1 Mass Model

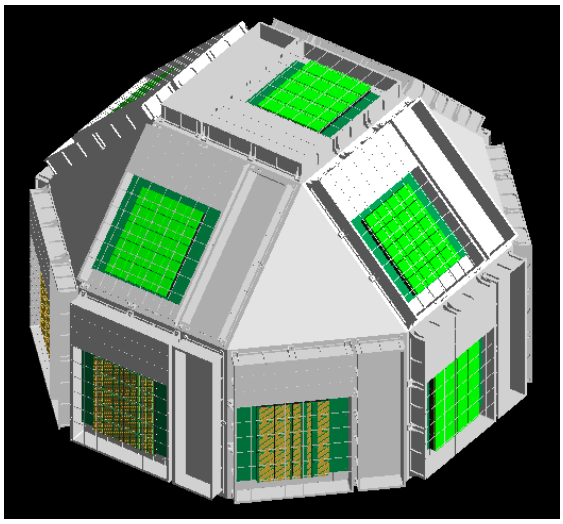

Figure 4: *The Daksha dome with* 13 *ME boxes mounted*

The Daksha mass model is used to realistically simulate the interaction of photons with the satellite and determine the counts received by every pixel of every detector onboard. The mass model is an accurate replication of the structure, geometry and chemical composition of the entire satellite. Simulations are done using GEANT4 (Agostinelli et al., 2003), a Monte Carlo simulation toolkit to simulate particle-matter interactions developed by CERN[1]. GEANT4 supports a diverse set of physical processes and interactions from the eV to GeV range, including support for polarised sources, customized source planes, energy spectra etc. Data from

[1]https://geant4.web.cern.ch/

these simulations is used to determine polarisation sensitivity and for developing and testing the polarisation pipeline.

4 X-Ray Polarimetry

4.1 Theory

X-ray detectors can directly measure the energies, intensities and position of energy deposition by X-rays. As polarisation cannot be measured directly, X-rays typically must undergo some interactions which convert it to some quantity that can be measured directly, like intensity or position.

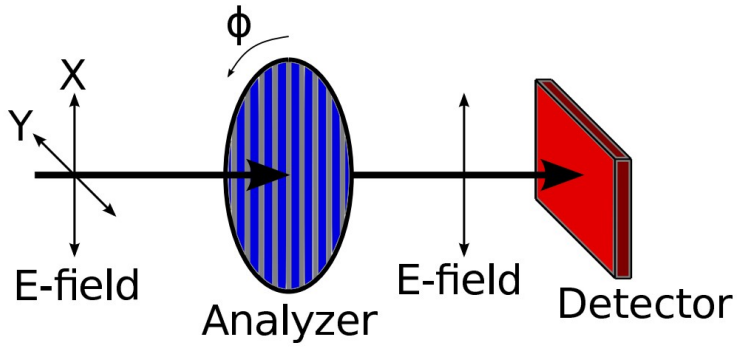

Figure 5: *Polarisation Analyzer : A linear polarisation analyzer is rotated and the associated detector records the intensity of photons (counts) at each angle as a modulation curve. Image Credit: Kaaret (2014)*

Consider a rotating polarisation analyser as shown in the figure above. As it is rotated, the intensity of photons detected varies. The resulting variation of photons vs. polarisation angle is known as the Modulation Curve, which can be written as

$$S(\phi) = A + B\cos^2(\phi - \phi_0) \tag{1}$$

where ϕ_0 is the polarisation angle at which maximum intensity is recorded. A describes the polarised intensity component, and B the unpolarised intensity. The typical way to analyse polarisation thus relies on finding this modulation curve by means of a physical process and fitting it to obtain the various parameters. As we will see soon, this method is ineffective for our application, which requires the development of a different approach.

4.2 Compton Polarimetry

4.2.1 Cross Section

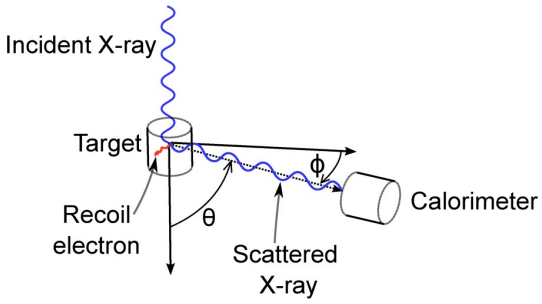

Figure 6: *A typical Compton polarimeter. Image Credit: Kaaret (2014)*

At energies above a few tens of keV, Compton scattering is the dominant interaction of X-rays with matter. When the X-ray energy is an appreciable fraction of the rest mass energy of an electron, the electron will recoil during the interaction, taking energy from the photon. The cross-section of scattering is given by the Klein-Nishina formula-

$$\frac{d\sigma_C}{d\Omega} = \frac{r_e^2}{2}\left(\frac{E'}{E}\right)^2\left[\frac{E'}{E} + \frac{E}{E'} - 2\sin^2\theta\cos^2\phi\right] \tag{2}$$

where r_e is the classical electron radius, E is the initial photon energy, E' is final photon energy (Lei et al., 1997).

4.2.2 Utilising the Cross Section

For scattering angles near 90°, the azimuthal distribution of the scattered photon is strongly dependent on the X-ray polarisation. This distribution can be shown to follow a modulation curve of the form shown in Equation 1. For on-axis sources therefore, fitting this azimuthal distribution is a straightforward way to estimate polarisation.

For off-axis sources (where $\theta \not\approx 90°$) however, such a fitting based approach is ineffective as it is no longer simple to fit the obtained distribution to Equation 2 for arbitrary θ, as the azimuthal scattering profile no longer follows a simple sinusoidal modulation curve due to the cross section being asymmetrical and pixel geometry. This is why a modulation curve-fitting based approach as done for AstroSat/CZTI (Chattopadhyay et al., 2019) is unsuitable for a mission like Daksha, where the

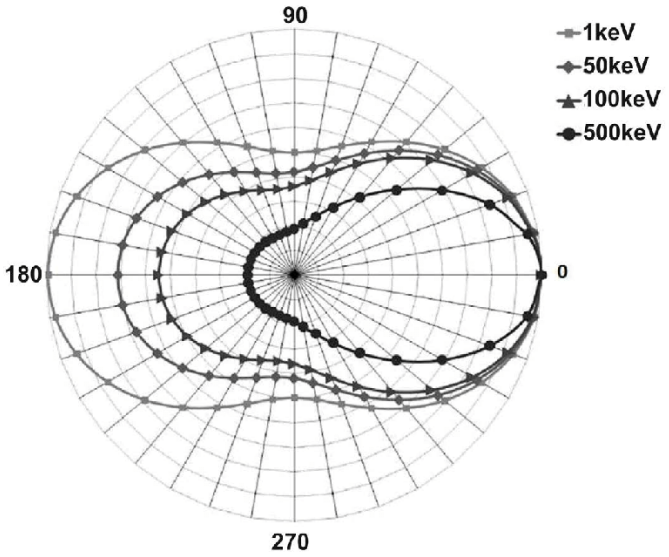

Figure 7: *Klein-Nishina cross section as a function of energy. Image Credit: Alzimami (2018)*

aim is to accurately constrain the polarisation of GRBs that occur all over the sky. A novel template matching based approach was chosen for this task in order to fully harness the many detectors onboard (Vaishnava et al., 2022).

4.3 Compton Polarimetry with Pixelated Detectors

With pixelated detectors, we cannot get a continuous distribution of counts with ϕ and only have information from discrete angular bins. The incident photon deposits a fraction of energy at the *incident pixel*, and a larger part of the energy is released as the scattered photon which is detected in a different pixel (*scattered pixel*).

4.3.1 Compton Scattering Events

To obtain the angular distribution of scattered photons, we treat scattering events occurring in specific pixels as occurring in discrete angular bins, and generate a histogram based off of that. This is shown in Figure 8. There are a few points to note here -

1. The detection of the Compton scattered photon is expected to occur at the same time as the detection of the incident photon since photon travel time is negligible. Such events are known as **double events**.

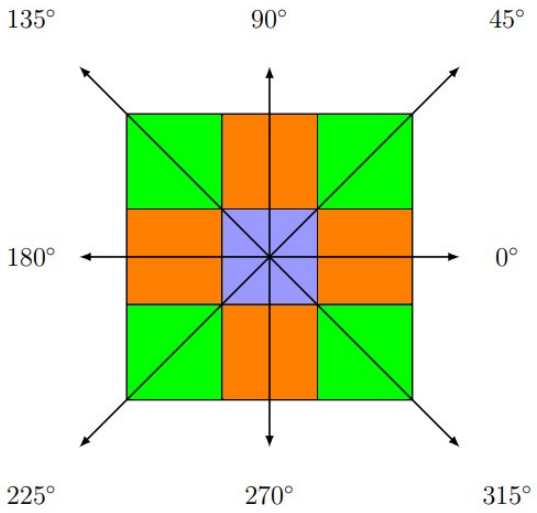

Figure 8: *Central pixel in purple and neighbouring pixels. Simultaneous events in these neighbouring pixels constitute a valid double event. Image Credit: Parth Sastry*

2. The Compton scattered photon is not expected to travel far from the scattering site before getting absorbed, so we only consider double events occurring within **adjacent pixels** to avoid the chance coincidence events that are going to occur (two independent photons arriving within a single detector clock cycle at different pixels).

3. Despite imposing the neighbouring pixel criteria, one still observes some chance coincidence events, and pairs caused by other processes (e.g. charge sharing, fluorescence etc.) and thus we impose a third criteria comparing the energies of the two events and imposing a limit on the total energy of the incident photon.

   For a true Compton scattering event, energy of the scattered photon is always greater than the recoil electron energy for incident photon energies < 280 keV. Furthermore, we only select incident and scattered photons lying within the energy range of $20-200$keV having total energy $100\text{keV} \leq E_{\text{tot}} = E_{\text{scattered}} + E_{\text{incident}} \leq 400\text{keV}$. These event energy criteria and total energy criteria help us make sure we only select true Compton Events (since Compton Scattering occurs mostly among medium energy X-Rays).

   For lower energy of the incident photons and scattering angles around 90°, the ratio of the energy of the scattered photon and the recoil electron is ≥ 2. This helps us to further weed out chance coincidence events from true scattering events.

To summarize - double events occurring in adjacent pixels (Figure 8) that satisfy the Compton Criteria are valid Compton events. Depending on which adjacent pixel the scattering occurred in, we assign this Compton event an angular bin ranging from 0° to 360° in increments of 45°. This gives us the observed angular distribution, or histogram of Compton events that are seen in our data. We add the histograms obtained from all Compton events for each ME box and add them to obtain a combined distribution.

All these results are taken from the PhD thesis of Dr. Tanmoy Chattopadhyay (Chattopadhyay et al., 2019) who was responsible for coming up with this pipeline to perform X-ray polarimetry with AstroSat/CZTI. The Daksha polarimetry pipeline that shall be described here was primarily developed by Parth Sastry as a part of his BTP, and my work has been related to further improvements and intensive testing of his codebase.

5 Methodology

5.1 Overview

As discussed in Section 4.2.2, a template matching approach was implemented to estimate the polarisation characteristics. This method relies on χ^2 fitting of the observed histogram ($H_{\mathrm{obs,i}}$) with a library of simulated template histograms ($H_{\mathrm{sim,i}}^{\mathrm{PA,PF}}$) generated for different combinations of PA and PF values.

$$\chi^2 = \sum_{i=1}^{8} \frac{\left(H_{\mathrm{obs,i}} - H_{\mathrm{sim,i}}^{\mathrm{PA,PF}}\right)^2}{\left(\sigma_{\mathrm{obs,i}}^2 + {\sigma^2}_{\mathrm{sim,i}}^{\mathrm{PA,PF}}\right)} \tag{3}$$

For our analysis we assume that ${\sigma^2}_{\mathrm{sim,i}}^{\mathrm{PA,PF}}$ is negligible, due to the method used to create the templates (see 5.2). The expression then becomes

$$\chi^2 = \sum_{i=1}^{8} \frac{\left(H_{\mathrm{obs,i}} - H_{\mathrm{sim,i}}^{\mathrm{PA,PF}}\right)^2}{\sigma_{\mathrm{obs,i}}^2} \tag{4}$$

We thus obtain an array of χ^2 values corresponding to all the possible PA, PF combinations. The minimum χ^2 is said to be the best fit, and the values of PA and PF that yield this value likely describe the true polarisation characteristics of the source.

This analysis is independently done for histograms of each of the 13 faces currently in the Daksha mass model, and joint fitting is done to utilise information from the best few faces in order to improve estimates.

5.2 Generating Templates

Templates are generated using GEANT4 simulations of the Daksha mass model. We use discrete monoenergetic simulations in the $100 - 1000$ keV range. For each energy, we simulate with an unpolarised beam and a fully polarised beam with 18 discrete PA values $0°, 10°, \ldots, 170°$. For each discrete energy we can thus obtain a 18 fully polarised histograms and an unpolarised histogram. These simulations are done with a beams of equal flux that encompass the entire dome of Daksha. The flux is chosen to be very high, in order to make the Poisson error in counts negligible.

However, these histograms need to be scaled down to the spectrum of a GRB (see 2.1) in order to create a template histogram that would resemble a GRB. Once the spectrum, intensity and duration of a GRB is known, we can find the expected number of counts that would be received at each of the discrete simulated energies. The obtained histograms can then be scaled down accordingly and the samples can be used to numerically integrate over the counts spectrum in order to obtain the final template histogram.

A histogram at any PF, PA can be linearly interpolated from the existing unpolarised and fully polarised histograms for that PA

$$H_i^{PF} = \mathrm{PF} \times H_i^{pol} + (1 - \mathrm{PF}) \times H_i^{unpol} \tag{5}$$

We use this to obtain template histograms with 100 equally spaced PFs between 0.00 and 1.00. This gives us template histograms for all combinations of 18 PA values and 100 PF values. However, the PA axis of this template grid is quite course, with 10° steps. The histograms must be further interpolated to obtain templates for intermediate PAs. The method of interpolation will be discussed in Section 6.

5.3 Simulating GRBs

In order to validate the processing pipeline, we need to check it against a GRB with known localisation, spectrum and polarisation properties. We need to simulate this GRB over the Daksha mass model and check if the estimated PA, PF match with the actual values. GEANT4 allows simulation of sources with a continuous

spectrum, and we use this to specify photon source beam with a spectrum dictated by Equation 2.1.

This simulated GRB is then be shined over the mass model with the correct source location, and histograms can be obtained for each of the 13 faces by applying the Compton criteria as discussed before.

5.4 Background

Analysis of the Daksha background show that the Cosmic X-Ray Background and its reflection from the Earth's atmosphere are the most dominant components of the background. For now, the background is estimated to be isotropic with an energy integrated photon rate of $\phi = 0.3565$ ph/cm^2/sr/s. A separate simulation is run in GEANT4 with a spherical isotropic source shining photons on the mass model with this rate. A large amount of photons are simulated, so that a background events file can be randomly sampled to give the expected background for a GRB with any duration. Thus we obtain histograms for the background, and add this to the raw GRB histogram to get a more realistic signal.

5.4.1 Background Subtraction

In the actual mission, background subtraction will take place by recording the counts for a larger duration before and after the burst. This will be representative of the background that will be persistent through the burst as well. The recorded background can then be downscaled to the duration of the GRB and then subtracted to approximately get rid of the background from the recorded signal.

In a simulation-based implementation, we sample events corresponding to 10 times the duration of the GRB from the background events file mentioned before, and scale this down to the duration of the GRB. This approach is approximately equivalent to what will happen on-board Daksha and the simulated background can then be subtracted from the simulated signal (that already contains a simulated background of its own). Care is taken to ensure both background samplings are done with different random seeds, as the signal background and simulated background can be correlated otherwise.

5.5 Template Fitting

Once we have the background-subtracted histograms for each face, they can be fitted against the templates created earlier. Every face is independently fitted against its corresponding template bank, and the 2D χ^2 array is obtained. In

order to combine information from multiple faces, the χ^2 arrays from the top 5 brightest faces are added together for joint fitting. The minima of the combined array gives us the estimated parameters.

The χ^2 values obtained can be plotted as a contour plot. Error estimates for PF and PA are obtained from two-parameter confidence levels for the χ^2 distribution with $\Delta\chi^2 = \chi^2 - \chi^2_{min} = 2.28,\ 4.61$ and 9.21 corresponding to 1σ, 2σ and 3σ confidence intervals (Vaishnava et al., 2022).

5.6 Results

We can see results of the template matching method in the form of two contour plots in Figure 10. These results are for two GRBs that were detected by AstroSat/CZTI. We observe how both detections are comfortably within the 1σ error contour, even though the first GRB is considerably fainter. For the brighter GRB, we get an extremely well constrained estimate even though the actual PF is quite low, and this technique is supposed to be ineffective for small PFs beyond a threshold. Both sources are also shining from quite distinct locations in the Daksha frame, and highly off-axis.

These plots are at least preliminary confirmation that Daksha is indeed a sensitive polarisation instrument over a very large part of the sky it sees. Additionally, we can see the background-subtracted histogram recorded and compare it with the selected template to directly check if the template is actually a good approximation.

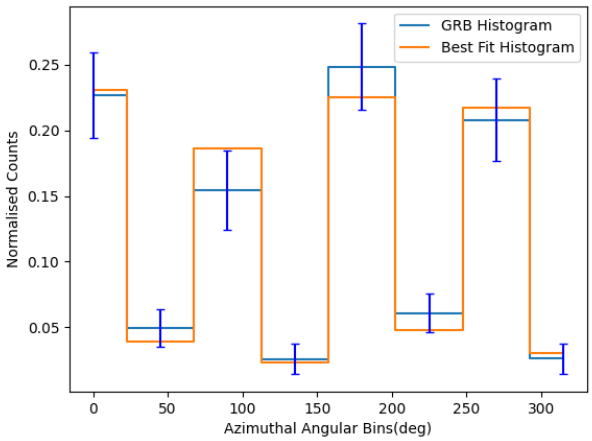

Figure 9: *Best fit histogram plotted over the processed GRB histogram*

We observe a good agreement between the two histograms, with the best fit counts mostly within 1σ error bars of the actual counts.

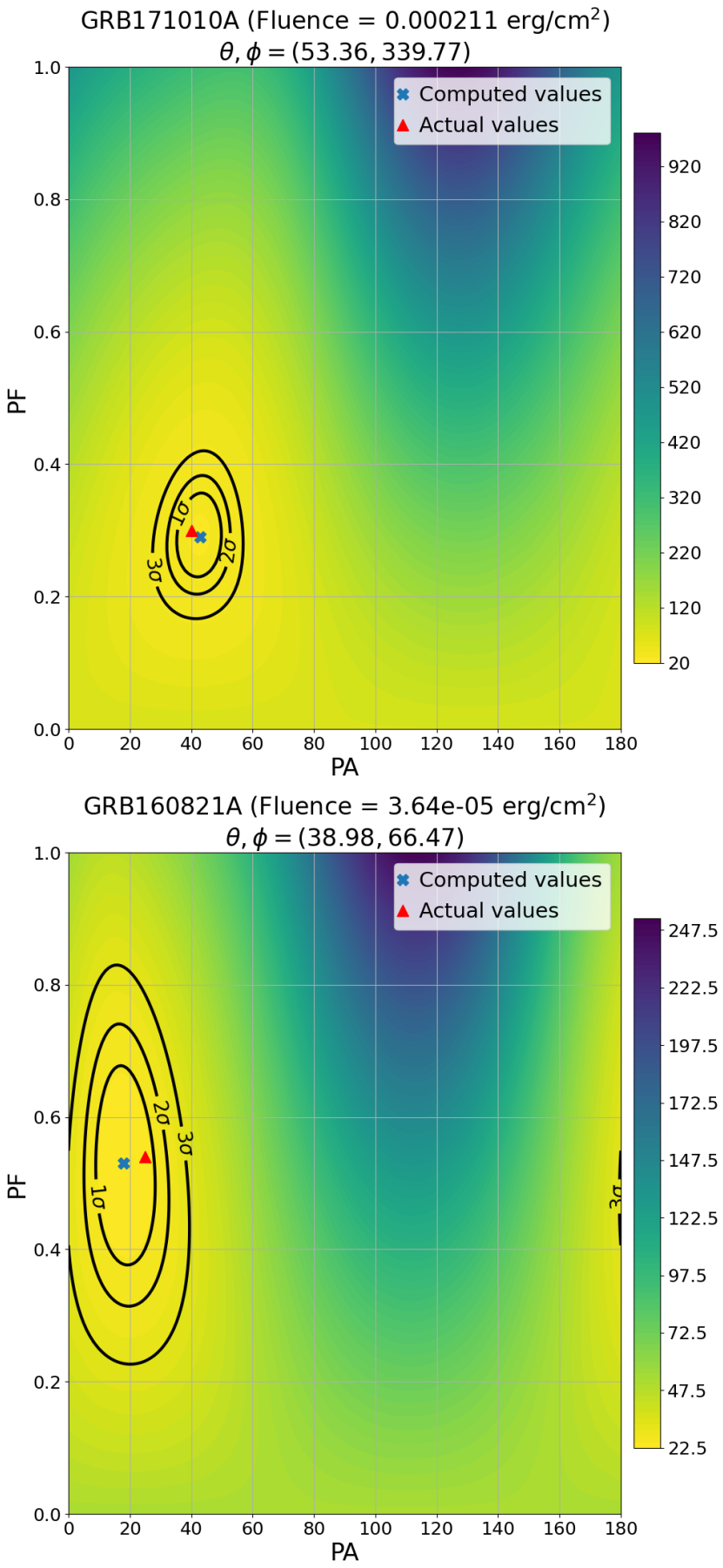

Figure 10: χ^2 Contour plots for two GRBs

6 Improvements

I discussed the process of generating templates in Section 5.2. I left the interpolation of the template bank along the PA axis for later, as it was one of the limitations of the original template matching implementation.

Originally, we assumed the variation of histograms with PA to be smooth, and used a cubic spline to interpolate a continuous function and sampled it to find counts at intermediate values. On examining the counts vs PA curve for a single bin of the histogram, we discovered that this method effectively overfits to noise and causes haphazard curves and inaccurate intermediate values for faces that received low counts.

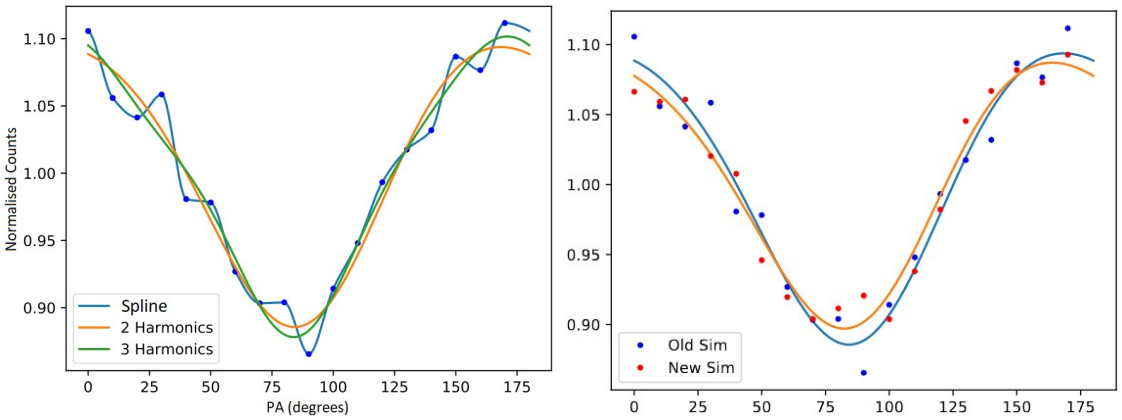

(a) *Comparison of different methods* (b) *2nd harmonic fits for distinct GRBs*

To combat this problem, we relied on fitting a function to the PA variation instead of naïvely interpolating. It is known that the variation is supposed to be approximately sinusoidal. Therefore, a harmonic fitting based approach was investigated, where we used the function

$$f(PA) = a_0 + \sum_{i=1}^{n} a_i \sin(2i \cdot PA + \phi_i) \tag{6}$$

To do a harmonic fit, we must therefore ascertain the parameters a_0, a_i and ϕ_i. We attempted this for $n = 2, 3, 4$ and empirically observed the best resulting curves for $n = 2$, and decided to replace spline interpolation with double harmonic fitting. This small change led to a visible improvement in contour plots we saw before, visible in Figure 12.

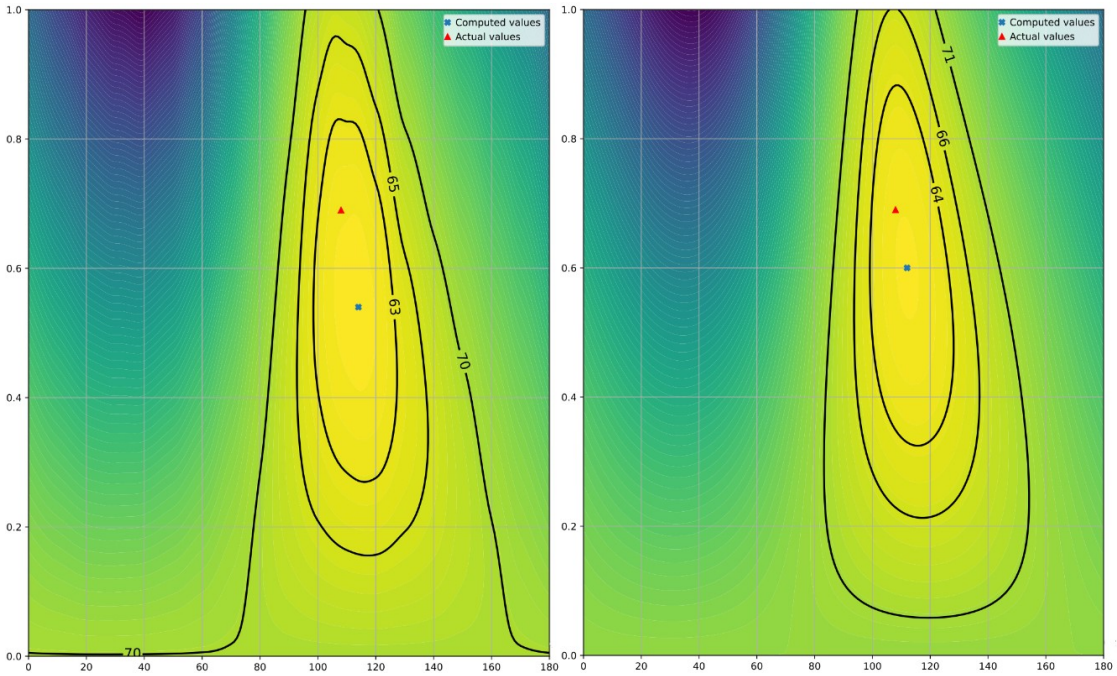

(a) With spline interpolation (b) With double harmonic fitting

Figure 12: *Double harmonic fitting yields better estimates and contours*

7 Minimum Detectable Polarisation

A more comprehensive measure of the polarisation sensitivity of an instrument is provided by the Minimum Detectable Polarisation or MDP. It is the minimum polarisation fraction that has only a 1% probability of being detected by chance (Weisskopf et al., 2010). In other words, if an unpolarised beam is shined upon the instrument, the measured polarisation will be less than the MDP 99% of the time. This metric imposes a rigorous quantitative limit on the polarisation sensitivity, as any source PF that is below the MDP cannot be confidently measured.

7.1 Methodology

In order to estimate the MDP of Daksha, a Monte Carlo based approach is used. This is different from the conventional approach that relies on an analytical expression (Kaaret, 2014). This method is only applicable to polarisation estimation methods that use modulation curve fitting, and depends on the parameters involved in Equation 1. Thus, even though this was used to quantify MDP of

AstroSat/CZTI (Vadawale, S. V. et al., 2015), this method cannot be used for Daksha. Therefore we take a brute-force approach that effectively simulates thousands of unpolarised GRBs, measures the PF for each and determines the 99th percentile value of the distribution obtained.

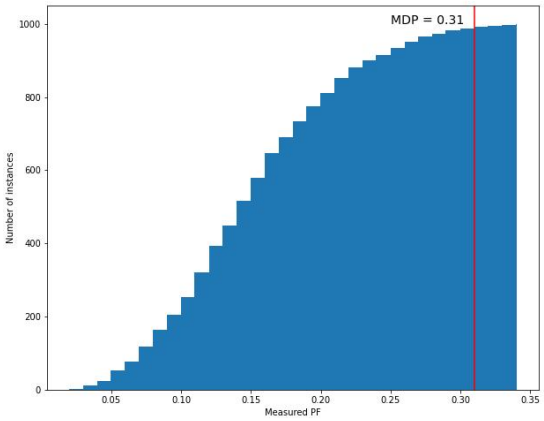

Figure 13: *A cumulative histogram for measured PF values with MDP labelled*

In order to implement this in practice, we simulate an unpolarised particle beam with a GRB spectrum and 1 billion photons using GEANT4. We then randomly sample the equivalent of $\tilde{1}000$ GRBs from this data, and obtain a PF distribution like the one in Figure 13.

7.2 Results

As an all sky GRB monitor, one of the goals of Daksha is to be sensitive to polarisation measurements for GRBs located all over the sky. In order to verify this, we must check if the MDP is similar for a diverse array of source locations. To confirm this, we used the method previously developed to find the MDP for 4 distinct sources and various fluence values. The results have been plotted in Figure 14.

We observe that the MDP is indeed consistent for all the directions throughout the tested fluence range.

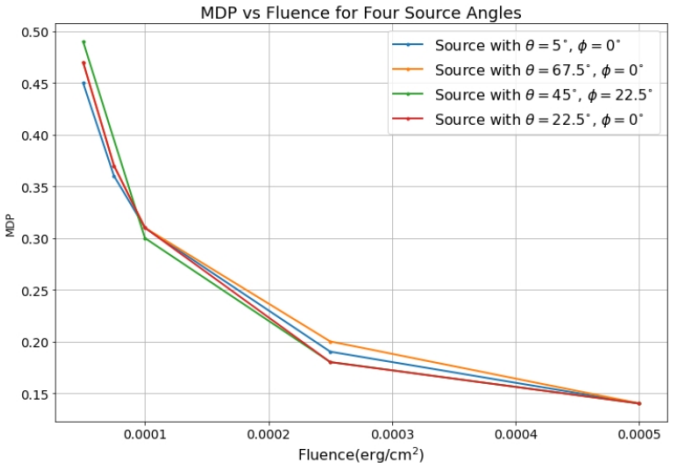

Figure 14: *MDP for sources from different directions with varying fluences*

7.3 Future Work

GEANT4 limits the maximum number of particles that can be simulated at once to 1 billion. But this number is too low to sample enough GRBs. For a fluence of 1×10^{-4} erg/cm^2, we would have to simulate at least 11 billion photons to get 5000 statistically independent GRBs! We are currently investigating a workaround to this problem, as both the simulation and MDP processing code are highly computationally intensive and each MDP calculation would take a lot of time this way.

8 Conclusion and Acknowledgements

With the analysis and testing phase of my project nearing its end, I need to focus on extensively documenting the code in order to make it simple to understand and execute for end users. This codebase will be likely to process real Daksha data later, hopefully in the very near future.

It was an honour to work with the Daksha team and contribute to this groundbreaking mission which will undoubtedly be an important milestone in Indian astronomy for decades to come. I would like to thank Dr. Sujay Mate, who has been my direct guide for this project and helped me learn everything from scratch and of course Prof. Varun Bhalerao for giving me the opportunity to work on this project as a part of STAR Lab and overseeing my progress every step of the way.

References

Agostinelli, S., Allison, J., Amako, K., et al. 2003, Nuclear Instruments and Methods in Physics Research Section A: Accelerators, Spectrometers, Detectors and Associated Equipment, 506, 250, doi: https://doi.org/10.1016/S0168-9002(03)01368-8

Alzimami, K. 2018, International Journal of Medical Physics, Clinical Engineering and Radiation Oncology, 07, 453, doi: 10.4236/ijmpcero.2018.74038

Band, D., Matteson, J., Ford, L., et al. 1993, The Astrophysical Journal, 413, 281, doi: 10.1086/172995

Chattopadhyay, T., Vadawale, S. V., Aarthy, E., et al. 2019, The Astrophysical Journal, 884, 123, doi: 10.3847/1538-4357/ab40b7

Grossan, B., Kumar, P., & Smoot, G. F. 2019, Journal of High Energy Astrophysics, 23, 14, doi: https://doi.org/10.1016/j.jheap.2019.08.001

Kaaret, P. 2014, The WSPC Handbook of Astronomical Instrumentation

Lei, F., Dean, A. J., & Hills, G. L. 1997, Space Science Reviews, 82, 309, doi: 10.1023/A:1005027107614

Vadawale, S. V., Chattopadhyay, T., Rao, A. R., et al. 2015, A&A, 578, A73, doi: 10.1051/0004-6361/201525686

Vaishnava, C. S., Mithun, N. P. S., Vadawale, S. V., et al. 2022, Experimental verification of off-axis polarimetry with Cadmium Zinc Telluride detectors of AstroSat-CZT Imager, arXiv, doi: 10.48550/ARXIV.2209.00222

Weisskopf, M. C., Elsner, R. F., & O'Dell, S. L. 2010, in Space Telescopes and Instrumentation 2010: Ultraviolet to Gamma Ray, ed. M. Arnaud, S. S. Murray, & T. Takahashi, Vol. 7732, International Society for Optics and Photonics (SPIE), 77320E, doi: 10.1117/12.857357